Available online at www.sciencedirect.com
ScienceDirect
Quaternary International 181 (2008) 15–31

Holocene palaeohydrology and climate variability in northeastern Spain: The sedimentary record of Lake Estanya (Pre-Pyrenean range)

Mario Morellón[a,*], Blas Valero-Garcés[a], Ana Moreno[a,b], Penélope González-Sampériz[a], Pilar Mata[c], Oscar Romero[d], Melchor Maestro[a], Ana Navas[e]

[a]*Instituto Pirenaico de Ecología (IPE)—CSIC, Campus de Aula Dei, Avda Montañana 1005, 50059 Zaragoza, Spain*
[b]*Limnological Research Center (LRC), Department of Geology and Geophysics, University of Minnesota, 2 20 Pillsbury Hall/310 Pillsbury Drive S.E. Minneapolis, MN 55455 0219, USA*
[c]*Facultad de Ciencias del Mar y Ambientales, Universidad de Cádiz, Polígono Río San Pedro s/n. 11510 Puerto Real (Cádiz), Spain*
[d]*Instituto Andaluz de Ciencias de la Tierra (IACT), CSIC—Universidad de Granada, Facultad de Ciencias, Avda. Fuentenueva, s/n, 18002 Granada, Spain*
[e]*Estación Experimental de Aula Dei (EEAD)—CSIC, Campus de Aula Dei, Avda Montañana 1005, 50059 Zaragoza, Spain*

Available online 4 March 2007

Abstract

This multi-proxy study of sediment cores from karstic Lake Estanya (Pre-Pyrenean Range, NE Spain) provides the first complete, continuous record of the hydrological evolution in the northeastern Iberian Peninsula over the last 9500 yr. Six sedimentary facies and four main sedimentary units have been defined after integration of sedimentological, mineralogical and geochemical analyses. The use of total sulphur content and sedimentary facies as paleohydrological proxies allows reconstruction of relative changes in lake level. The Estanya record shows a large increase in water availability after 9.2 ka, fluctuating lake levels and salinity during the period 9.2–4.2 ka; and generally higher lake levels after 1.7 ka. Periods of increased run-off and sediment delivery and less saline conditions occurred at 8.5–8.2, 6.7–5.9, and 4.9–4.2 ka. Dominant lower lake levels and concentrated waters during the period 4.2–0.8 ka were punctuated by a higher lake level, higher clastic input episode ca. 1.7–1 ka. Fluctuating, but higher lake levels occurred during the last 800 years. The main hydrological phases in Lake Estanya are coherent with Western Mediterranean and North Atlantic Holocene reconstructions, but they also show similarities with northern African records.

1. Introduction

Although the Holocene has been traditionally considered as a climatically more stable period than the Late Glacial, it is now clear it has been punctuated by rapid oscillations (Magny et al., 2002; Magny et al., 2004; Mayewski et al., 2004; Duplessy et al., 2005), which had a particular impact in the hydrological cycle at mid and low latitudes (Gasse, 2000). In Mediterranean regions the hydrological cycle has experienced large fluctuations during the Holocene, and shows evidence of a threshold response even to gradual forcing from changes in the Earth's orbital configuration and solar insolation (Liu et al., 2006). Many records from the Mediterranean and northern Africa suggest wetter conditions during the early Holocene and a progressive aridification after 5.5–4.5 ka BP (Magny et al., 2002), although exceptions to this pattern are numerous and many sites show a more complex evolution (Davis et al, 2001; Roberts et al., 2001a). Superimposed on the orbitally driven climate evolution, there are numerous rapid millennial-scale changes that have been correlated with the North Atlantic Bond Cycles (Bond et al., 1997, 2001). The abrupt onset and end of these hydrological fluctuations is linked to feedbacks between changes in insolation, oceanic and atmospheric circulation, hydrological cycles and vegetation cover (Gasse, 2000; Hu and Neelin, 2005), but their meaning is still poorly understood.

A number of arid and humid phases during the Holocene in mid-Europe and the western Mediterranean have been reconstructed using pollen data and a comparison between modern and fossil pollen spectra (Jalut et al., 2000), lake

*Corresponding author. Tel.: +34 976716142; fax: +34 976716019.
E-mail address: mariomm@ipe.csic.es (M. Morellón).

1040-6182/$ - see front matter © 2007 Elsevier Ltd and INQUA. All rights reserved.
doi:10.1016/j.quaint.2007.02.021

level, glacial advances (Magny et al., 2002; Magny, 2004), and fluvial evolution (Macklin et al., 2006). Although there are some chronological uncertainties and some differences in interpretations (Jalut et al., 2000; Magny et al., 2002; Magny, 2004) it seems that during these centennial to millennial scale cooler and wetter periods, lake levels rose, glaciers advanced and fluvial activity increased. Mayewski et al. (2004) analysed 50 globally distributed paleoclimate records and found six events of rapid climatic change during the periods 9.0–8.0, 6.0–5.0, 4.2–3.8, 3.5–2.5, 1.2–1.0 and 0.6–0.1 ka BP. Most of them are characterized by polar cooling and tropical aridity, except the last one that showed increased moisture at the tropics. However, more records are needed to test the timing and regional extent of these events and the millennial-scale cyclicity during the Holocene.

In the Iberian Peninsula, most of the paleoclimate reconstructions for the Holocene are based on pollen changes and they do not have the accurate chronology to capture all the high-frequency hydrological changes (p.e. Pons and Reille, 1988; Pérez-Obiol and Julià, 1994; Peñalba et al., 1997). Most pollen-based climate reconstructions from Spain show an early Holocene rapid transition to vegetation dominated by temperate deciduous woodland, a maximum forest development during the Mid Holocene, and a transition during the Late Holocene to the current drought-adapted vegetation (Pérez-Obiol and Julià, 1994; Burjachs et al., 1997; Carrión, 2002). New multiproxy records from the Iberian Peninsula during the last decade have changed our views on Holocene history from a generally benign climate punctuated by dry Mid Holocene period and an amelioration afterwards, to a complex fluctuation of arid and humid periods with an increased effective moisture during the Late Holocene (Allen et al., 1996; Valero-Garcés et al, 2000b; Luque Marín, 2003; González-Sampériz et al., in press). Several arid/humid transitions during the early (about 8 ka), mid (5 ka) and Late Holocene (4–3 ka) occurred in most sites. However, to reconstruct the effective moisture history of the Iberian Peninsula, long, high resolution, multiproxy, well-dated records from hydrologically sensitive regions are needed.

In this paper, we present a Holocene environmental and paleohydrological reconstruction based on sediment cores from Lake Estanya, a 20 m water depth karstic lake in the Pre-Pyrenean region. Records from Pyrenean glacial lakes have reconstructed vegetational history during Late Glacial and Holocene (González-Sampériz et al., 2006), and records from saline lakes in the Ebro Basin (Davis, 1994; González-Sampériz et al., in press) some of the main hydrological changes during the Holocene, although these records have numerous hiati and they are not continuous. The Estanya site provides the first continuous Holocene record in the region and shows large hydrological variations that help to understand climate evolution and to test the impact of rapid climate change in the Western Mediterranean, such as the effects of the 9000–8000 and the 4200–3800 cal yrs BP events.

2. Regional setting

2.1. Site location

The 'Balsas de Estanya' (42°02′N, 0°32′E; 670 m. a. s. l.) is a karstic lake complex located at the foothills of the Sierras Exteriores, the External Pyrenean Ranges (Martínez-Peña and Pocoví, 1984). The External Pyrenean Ranges are composed of E–W trending folds and thrusts composed of the Mesozoic formations. The outcropping of Upper Triassic carbonate and saline evaporite formations along tectonic structures has favoured the karstification processes and the development of large poljes and dolines (IGME, 1982). The Balsas de Estanya are located in a relatively small basin of 121.09 ha (Manuel López-Vicente, pers. commun.) (Fig. 1) that belongs to a larger Miocene polje structure (Sancho Marcén, 1988a). The karstic system contains four dolines holding water (7, 12, 20 m water depth and a seasonally flooded one) and a number of depressions already filled with sediments. Upper Triassic gypsiferous marls constitute the lake substrate whereas Muschelkalk limestones and dolostones outcrops constitute the highest reliefs of the catchment (Sancho Marcén, 1988b). Slope and alluvial deposits occur through the northwestern and southeastern littoral areas and colluvial deposits are located at the northern boundary of the drainage basin (Manuel López-Vicente, pers. commun.).

2.2. Climate and vegetation

The region has a Mediterranean continental climate with long summer drought (León-Llamazares, 1991). The mean annual temperature is 14 °C ranging from 4 °C (January) to 24 °C (July). Mean annual rainfall is 470 mm and mean annual evapotranspiration rate has been estimated as 774 mm (Meteorological Station at Santa Ana Reservoir, 17 km southeast of the lake). July is the driest month with an average rainfall of 18 mm and October is the most humid month (50 mm) (Fig. 2). Most of the precipitation is related to Atlantic fronts during the winter months, although meso-scale convective systems produce large precipitation during the summer (García-Herrera et al., 2005). As in most of northern Spain, winter rainfall has a strong correlation with NAO index (e.g., Zorita.et al., 1992; Hurrell, 1995; Trigo and Palutikof, 2001; Muñoz-Díaz and y Rodrigo, 2003). An extreme negative mode of the NAO with high pressure over the Icelandic area and low in the Azores produces a blocking situation for the westerlies, and a southward displacement of storm tracks. As a result, low temperatures and below-normal precipitation over central and northern Europe, and above-normal precipitation over southern and central Europe, the Iberian Peninsula and northwestern Africa occur.

The Estanya lakes are located at 670 m. a.s.l. at the boundary between the *Buxo-Quercetum rotundifoliae* and the *Violo-Quercetum fagineae* forest communities that corresponds to the transition zone between the Mediterranean

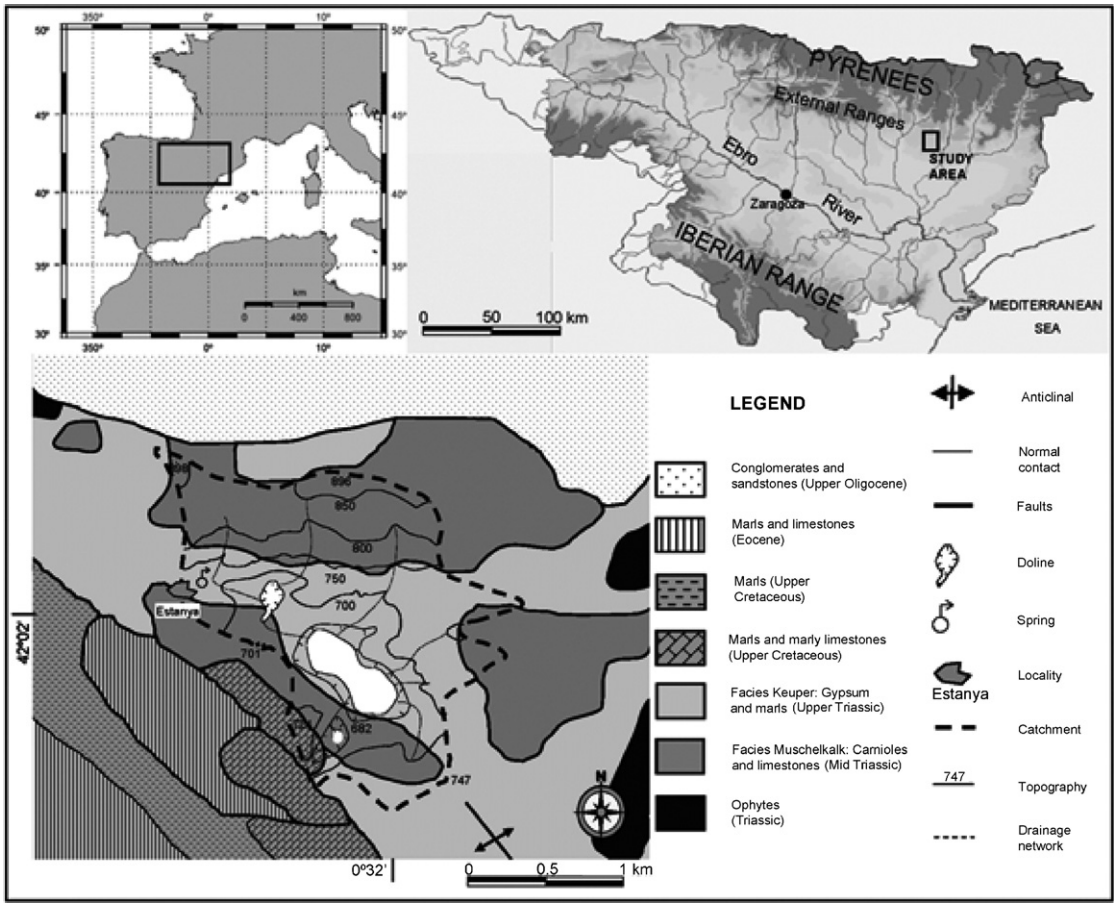

Fig. 1. Geographical location map of the study area in the Iberian Peninsula. Geological map of Lake Estanya surrounding area. Drainage area and main springs are also indicated.

and Submediterranean bioclimatic regimes. (Rivas-Martínez, 1982). The first community is a sclerophyllous woodland dominated by evergreen oak (*Quercus rotundifolia*) with some *Buxus sempervirens, Juniperus oxycedrus* and submediterranean plants. The second plant community is dominated by dry-resistant deciduous oaks (*Quercus faginea* and *Q. cerrioides*) with some *B. sempervirens* (Peinado Lorca and Rivas-Martínez, 1987).

2.3. Hydrology and limnology

The main lake basin, 'Estanque Grande de Abajo' (42° 02′N, 0° 32′E, 670 m a.s.l.), is '8-shaped', composed of two sub-basins with maximum depths of 12 and 20 m and very steep margins (Ávila et al., 1984). These two sub-basins are separated by a sill, 2–3 m below present-day lake level, only emerged during long dry periods, e.g. in 1994–1996 drought (see Fig. 2: b,c,e). Total lake surface is 188,306 m^2 (maximum length is 850 m and maximum width is 340 m). Total volume has been estimated as 983,728 m^3 (Ávila et al., 1984). Current hydrology of the Estanya lakes is mostly controlled by groundwater inputs and evaporation output. Calculated evapotranspiration (Meteorological Station at Santa Ana Reservoir, 17 km southeast) exceeds rainfall in about 300 mm/yr. Runoff is small, and there is no permanent inlet. However, alluvial fan deposits occur at the northwestern and southeastern shorelines, revealing episodic flow activity of the creeks (López-Vicente, pers. commun.). There is no surface outlet. The lake is mainly fed by groundwater from the surrounding local dolostone aquifer, related to the hydrogeological system of the Estopiñán Synclinal (García-Vera, 2004). A permanent spring is located at the north end of the polje, and several ephemeral small springs occur in the watershed. Subaqueous springs also discharge in the lake. The substrate, composed of non-permeable Upper Triassic Keuper facies, limits groundwater losses. There are no available groundwater and lake level data to calculate the hydrological balance in the lake. However, the response of the system to precipitation is relatively rapid, as indicated by about 1 m lake level drop during the relatively dry year 2005, and by several metres decrease during the last long dry period 1994–1996 when the central sill separating both sub-basins emerged (Fig. 2: b,c and e).

The lake is monomictic, with thermal stratification extending from March to September, and a thermocline located between 5 and 10 m deep (Ávila et al., 1984). Water chemistry is dominated by sulphate (1813.1 $mg\,l^{-1}$) and

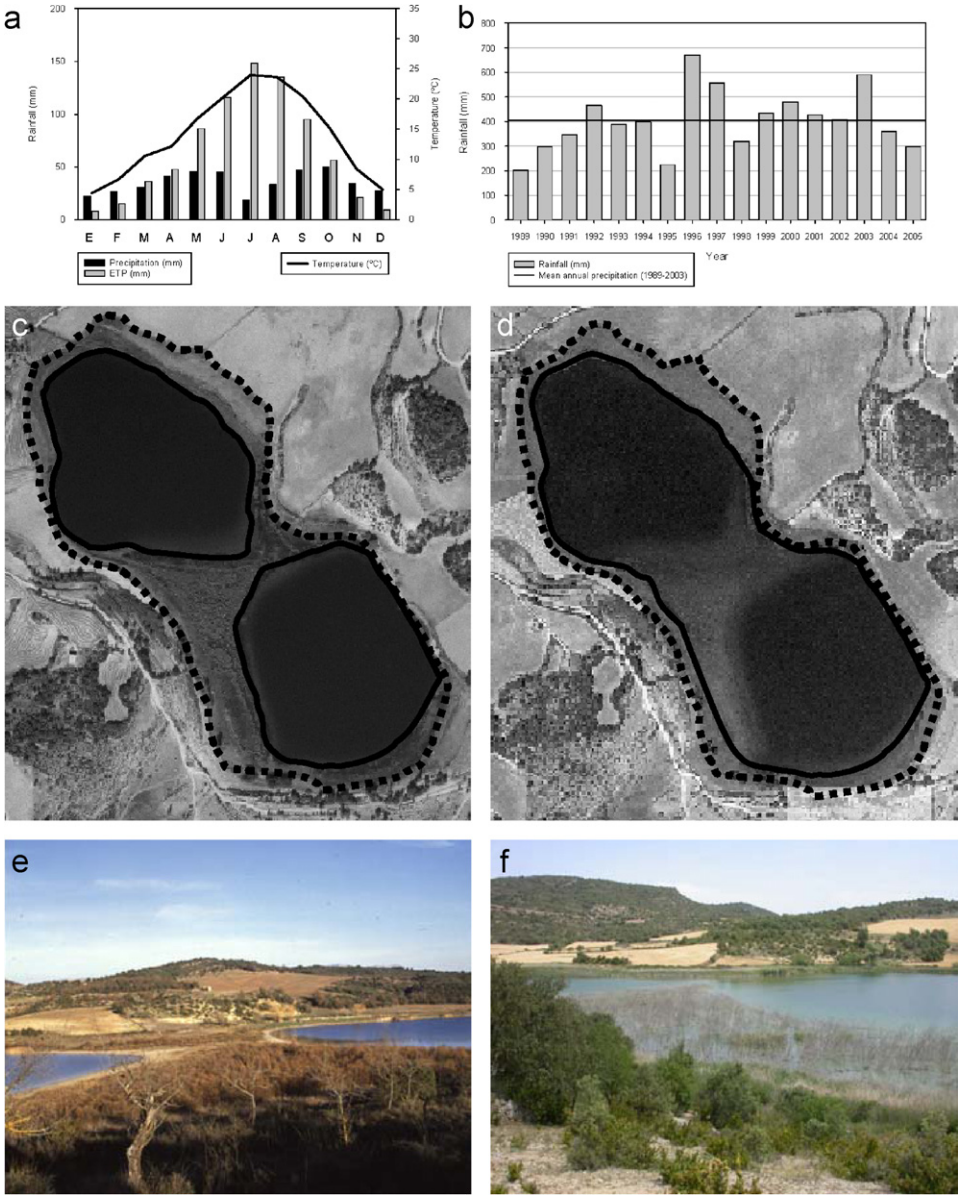

Fig. 2. (a) Mean monthly rainfall (mm), potential evapotranspiration (ETP, mm) and temperature (°C) at the Santa Ana reservoir. (b) Mean annual rainfall during the period 1991–2005. *Source*: Ebro Basin Watershed Authority (CHE). (c and e) The Estanya lakes in 1996 during a dry period when the sill emerged and lake level lowered more than 3 m. (d and f) The Estanya lakes in 2006 during a period of relatively high lake level. In aerial photographs (c and d), dotted lines represent the external limits of littoral vegetation belt, whereas continuous lines represent shorelines for years 1996 and 2006, respectively.

calcium (400 mg l^{-1}) and conductivity is 3280 μS. Values of alkalinity range from 2 to 3.5 meq l^{-1} and pH is about 8 (Ávila et al., 1984). Vertical profiling in June 2005 revealed thermal stratification with thermocline located at 7 m water-depth. Anoxic conditions were also detected at the hypolimnion (Table 1). The lake margins are occupied by a vegetation belt of *Typha angustifolia, Typha latifolia, Phragmites australis, Juncus* ssp. and *Tamarix* ssp. (Ávila et al., 1984).

There is no morphological evidence of former higher lake level terraces. However, lake sediments occur up to 1 m above present-day lake level in the SE margin and some flat areas in the S margin could correspond to erosive terraces. The lake basin comprises mainly two modern depositional environments: littoral platform and off-shore, distal. The talus is very steep, and there are seismic evidences of mass-wasting deposits, particularly in the northern shore of the southern sub-basin. The littoral platform environments are not well developed because of the steep margins of the basin. The narrow marginal platforms and the sill between the two sub-basins are colonized by hydrophytes/submerged macrophytes and charophytes. They buffer littoral waves, stabilise the substrate, provide support for epiphytic fauna, and largely contribute to the production of carbonate particles. Current conditions show a low-energy environment with small lake level fluctuations (2–3 m).

Table 1
Physical and chemical properties of the Estanya Spring and Lake Estanya (deepest sub-basin) for 24 June 2005

Sample	Water depth (m)	Temperature (°C)	Conductivity ($\mu S\,cm^{-1}$)	pH	Oxygen saturation (%)	Mg	K	Na	Sr	Li ($mg\,l^{-1}$)	Ca	HCO_3	Cl	SO_4
Estanya spring	—	14.0	627	7.64	100.0	12.7	1.7	20.5	0.23	0.11	55.3	0.3	1.2	48.5
Lake Estanya	0	24.3	3440	7.63	65.8	132	14.2	133	7.8	0.16	440	1.37	6.6	1813.1
Lake Estanya	16	5.1	3330	7.39	0.0	127	14	124	7.1	0.15	402	1.49	6.3	—

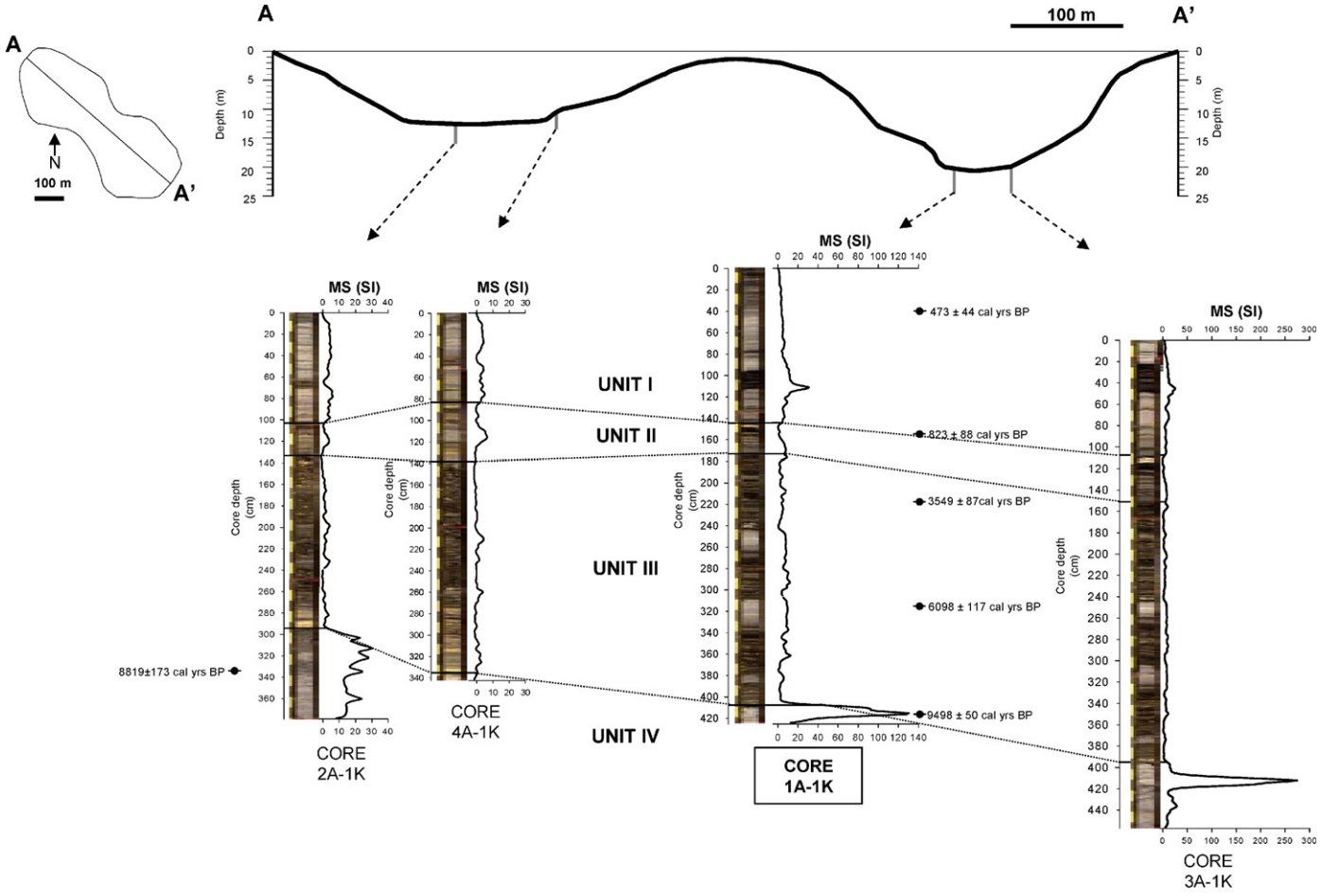

Fig. 3. Location of the four cores retrieved in Lake Estanya. Core images are accompanied by their MS curves (in SI units) and dotted lines represent core correlations of the main sedimentary units. Calibrated ages (in cal yr BP) are also indicated at their respective core depths.

3. Materials and methods

The Balsas de Estanya watershed was identified and mapped using available topographic and geological maps. A seismic survey conducted with a 3.5 Khz seismic profiler in June 2002 revealed a lacustrine sequence of >15 m in both sub-basins of the Estanya Lake. In spring 2004, sediment cores were retrieved in the deepest areas of both sub-basins using modified Kullenberg piston coring equipment and platform from the Limnological Research Centre (LRC), University of Minnesota (Fig. 3). Physical properties were measured by a Geotek multi-sensor core logger (MSCL) every 1 cm in all the cores before opening them. The cores were split in two halves and sedimentary facies were defined by macroscopic visual description including colour, grain-size, sedimentary structures, fossil content, and by microscopic smear slide observations. All cores were correlated using sedimentary facies and magnetic susceptibility. Cores were imaged with a DMT core scanner.

Large-format thin sections (120 mm × 35 mm) were prepared after freeze-drying and subsequent impregnation

Table 2
Calibrated radiocarbon dates obtained in the Lake Estanya cores 1A–1K and 2A–1K

Core	Core depth (cm)	Laboratory code	^{14}C AMS age (BP)	Calibrated age (cal BP) (range 2σ)	Type of sample	Calibration
1A–1K	39.5	Poz-12245	405±30	473±44	Plant remains and charcoal	INTCAL04
	155	Poz-12246	895±35	823±88	Aquatic plant root	INTCAL04
	218	Poz-12247	3315±35	3549±87	*Salix* leave	INTCAL04
	315.5	Poz-12248	5310±60	6098±117	*Graminea* seed	INTCAL04
	417.5	Poz-9891	8510±50	9498±50	Wood fragment	INTCAL04
2A–1K	334.5	Poz-9810	7960±50	8819±173	Wood fragment	INTCAL04

These dates were calibrated using CALIB 5.1 software and the INTCAL04 curve (Reimer et al., 2004); and the mid-point of 95.4% (2σ probability interval) was selected.

with epoxy resin (Araldite) under vacuum conditions (Brauer et al., 2000). Microscopic inspection at 100× magnification of selected samples provided qualitative information about sediment components and texture of the sedimentary facies. Thin-section images were obtained with a digital camera (Carl Zeiss Axiocam) and the software Carl Zeiss Axiovision 2Æ0. (Brauer et al., 2000; Mangili et al., 2005).

The longest core (LEG04-1A-1 K) retrieved in the deepest sub-basin (Fig. 3) was sub-sampled every 2 cm for total organic carbon (TOC), total inorganic carbon (TIC), total nitrogen (TN) and total sulphur (TS) and every 5 cm for mineralogy and biogenic silica (BGS) analyses. TC, TS and TOC contents were measured with a LECO SC 144 DR elemental analyser. For TOC analyses, carbonates were removed by adding 1:1 HCl. TN content was analysed by a VARIO MAX CN elemental analyser.

Bulk sediment mineralogy was characterized by X-ray diffraction using a Phillips PW1820 diffractometer, CuK_α radiation, graphite monochromator and automatic slit. Relative mineral abundance was determined using peak intensity, following a standard procedure (Chung, 1974a, b). Accordingly, the intensity of the main peak of every mineral (in counts) obtained with Brucker D8 advance software has been corrected according to the factors calculated for each mineral in the diffractometer and used for quantification procedures. Scanning Electron Microscopic study was carried out using a ESEM FEI-Quanta 200 and SIRION FEG coupled with an energy dispersive X-ray (EDAX) for elemental identification. Samples were carbon-coated to avoid peak overlapping. SEM observations were made both in conventional SEM mode and low vacuum mode to avoid charge and collapse of organic structures.

Biogenic silica (opal) content was analysed following an automated leaching method (Müller and Schneider, 1993) by alkaline extraction (De Master, 1981). The opaline material was extracted with 1 M NaOH at 85 °C in a stainless steel vessel under constant stirring, and the increase in dissolved silicawa continuously monitored. For this purpose, a minor portion of the leaching solution was cycled to an autoanalyzer and analysed for dissolved silicon by molybdate-blue spectrophotometry. The resulting absorbance versus time plot was then evaluated according to the extrapolation procedure of De Master (1981).

The chronology for the lake sequence is constrained by five accelerator mass spectrometry (AMS) ^{14}C dates from LEG04-1A-1K core and one from LEG04-2A-1K analysed at the Poznan Radiocarbon Laboratory (Poland) (Table 2).

4. Results

4.1. Chronological model

To construct the age model of the Estanya sequence, the six radiocarbon dates listed in Table 2 were used. The sediment/water interface was not preserved in core LEG04-1A-1K, but the upper part of the sequence was reconstructed using a short core and correlation between the two cores was performed using TOC/OM and TIC/carbonate values (Fig. 4). The upper 22 cm of the short core were added to LEG04-1A-1K to complete the sequence. The sedimentation rate during the lower and mid part of the record is about 0.3 mm/yr, but it increases up to 2.3 mm/yr during the last 800 years (Fig. 4). This abrupt increase coincides with a change in sedimentary facies that indicate increased erosion in the catchment. A similar increase in sedimentation rates was reported from a previous littoral core by Riera et al. (2004). The Estanya record described in this paper spans from 9498±50 cal yrs BP to present.

4.2. The sedimentary record

4.2.1. Sedimentary facies

The 430 cm long core 1A–1K from the deepest area (20 m) of the SE sub-basin of Lake Estanya is composed of alternating: (i) clastic, banded, carbonate silty and muddy facies, and (ii) laminated, organic-rich facies with gypsum and carbonate laminae (Fig. 5). Clastic facies are composed of allogenic (i.e., detrital) material derived from weathering and erosion of the soils and bedrock of the watershed transported to the lake by fluvial, sheetwash, gravity, or aeolian processes and endogenic material (*Chara*

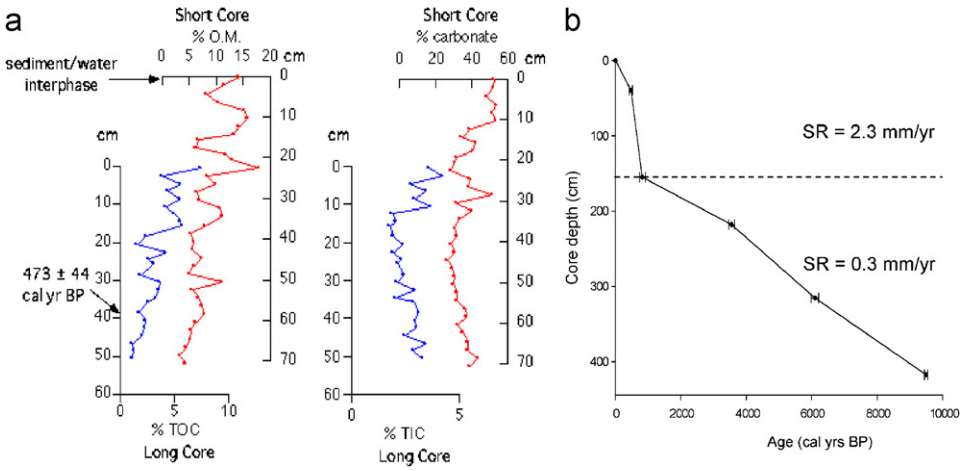

Fig. 4. (a) Correlation between the short core and the long core (1A–1K) using of the percentage of organic matter and calcium carbonate (short core) and TOC and TIC (long core); (b) Chronological model of the studied sequence based on the linear interpolation of 5 AMS ^{14}C dates. Averaged sedimentation rate for two distinct intervals is indicated.

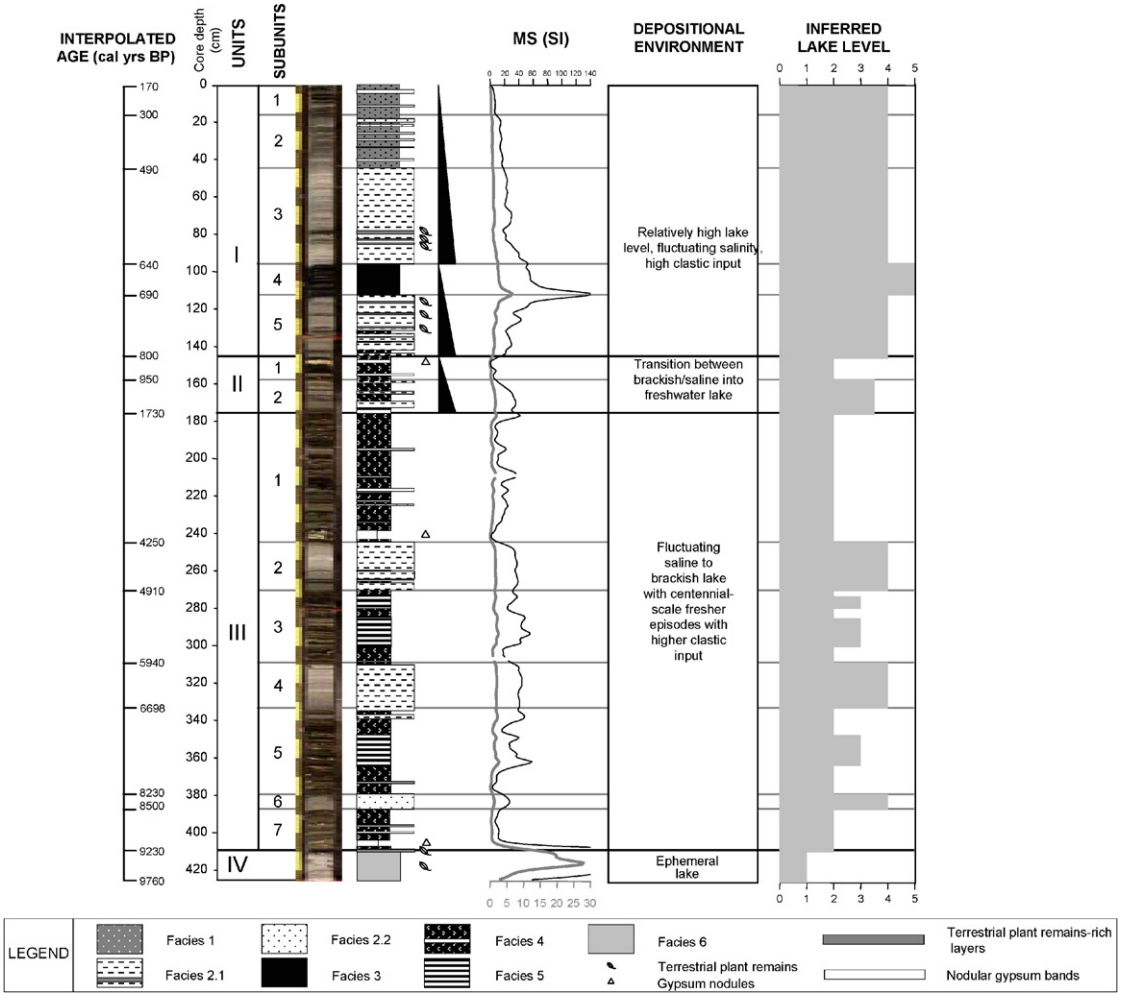

Fig. 5. Digital image, lithological column and magnetic susceptibility profile from Core 1A–1K. The four lithological units are accompanied by a brief interpretation of their depositional environments and an estimation of the inferred lake level, represented by horizontal bars (from 1 to 5) for each sedimentary Subunit according to facies interpretation (1: Ephemeral lake; 2: Saline lake; 3: Brackish lake; 3.5: Brackish to freshwater lake transition; 4: Freshwater lake; 5: Meromictic freshwater lake). The interpolated dates for the boundaries of the lithological Subunits are indicated. A detailed facies legend is shown.

fragments, micrite peloids, carbonate coatings) reworked from the littoral carbonate-producing environments. XRD analyses revealed that clastic intervals are composed by clay minerals, calcite and quartz, with minor amounts of dolomite, feldspars, high-magnesium calcite (HMC), pyrite and occasional gypsum and aragonite. Laminated, organic-rich facies comprise gypsum-rich sapropels and finely laminated intervals including laminae composed of bacterial–algal mats, diatoms, endogenic carbonate (aragonite, calcite, dolomite) laminae, gypsum, and clay-rich laminae (Fig. 6). Gypsum nodules are also common in some levels and they are interpreted as formed during the early diagenesis once the sediment was deposited.

Six sedimentary facies have been identified after integration of visual description, microscopic observation of smear slides following Schnurrenberger et al. (2003) procedures, thin sections, mineralogical analyses (XRD) as well as SEM observations and elemental geochemical proxies (Table 3, Fig. 5).

4.2.2. Magnetic susceptibility record

The MS values in the Estanya core are generally low (about 5 SI units) corresponding to the range of paramagnetic materials expected in carbonate, organic and evaporite-rich sediments. They remain constant throughout most of the sediment record, except at the lowermost part of the sequence (130.4 SI) and one peak at the interval 112.5–94.5 cm (30.1 SI) (Fig. 5). MS values responds to facies distribution. Relatively high and constant values averaging 7 SI, correspond to clastic facies 1 and 2, whereas organogenic facies 4 and 5 show an irregular pattern although usually lower values (around 4 SI). The general MS curve follows the quartz content curve (Fig. 7). Clay minerals content has the same pattern but at the uppermost part of the sequence (after the upper MS peak, from 111.5 cm to top), both quartz and phyllosilicates curves diverge (as quartz content and MS values decreases, clay mineral content increases (Fig. 7)). Increasing clay minerals content accompanied by decreasing quartz content reflect a decreasing grain-size trend which likely influences MS values. Thus, MS is used primarily as an indicator of clastic, allogenic content in sediments derived from the watershed.

Higher-magnitude, ferrimagnetic-scale peaks are recorded within facies 3 and facies 6, likely indicative of exceptional conditions. X-ray diffraction did not reveal bulk mineralogy differences that might explain these excursions in MS values. The variations must, therefore, reflect subtle changes in magnetic content due to either mineralogy or particle size distribution (Anker et al., 2001). Rutile (TiO_2) grains have been identified by SEM observations. It may indicate that titanomagnetite (which yields strong magnetic signal) may be present in the sediment sequence. Formation of magnetic minerals in soil may have also contributed to the high MS values at the base of the core.

Black colour in the massive fine grained sediments of facies 3 are not caused by significantly higher organic matter content, but by the presence of fine-grained sulphides. It has to be noted that facies 3 only occurs in cores from the SE sub-basin, deeper (20 m) than NW sub-basin (12 m), where meromictic conditions are more likely. The high MS peak may be related to high content of fine-grained iron-bearing minerals from the surrounding soils delivered to the centre of the lake during a period of more intense erosion.

4.2.3. Geochemical proxies: TOC, TIC, TN, TS, BGS

TOC is one of the main criteria to characterize sedimentary facies in the Estanya core: organogenic facies (facies 4 and 5) are characterized by high values (6.6% and 12.7% on average) and clastic facies (facies 1, 2, 3 and 6) by

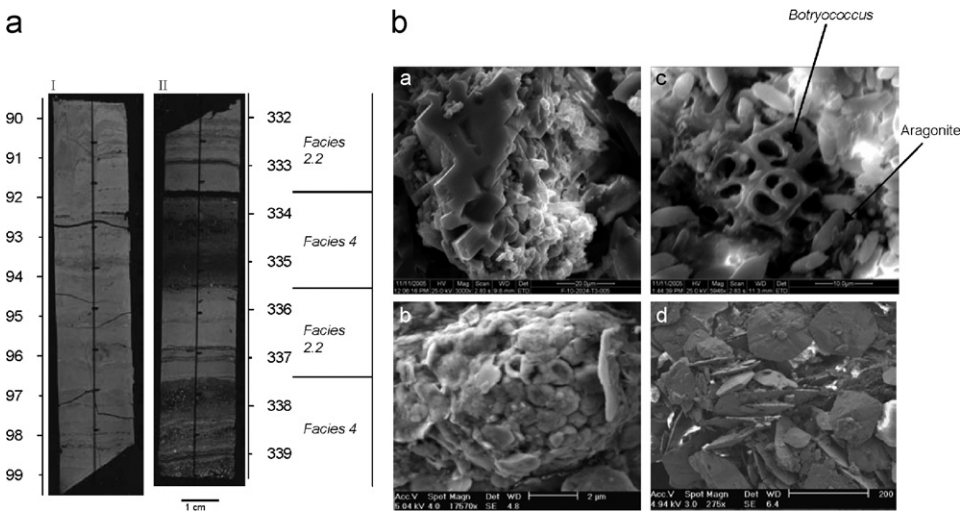

Fig. 6. (a) Thin sections of facies 2.2 and facies 4. (b) SEM pictures of variegated, laminated facies (Facies 5): (a) skeletal gypsum, (b) *Botryococcus* mats with aragonite grains; (c) pyrite framboid and (d) lenticular gypsum.

Table 3
Main sedimentological features, mean geochemical composition (TOC, TN, TOC/TN ratio and TS) and interpreted depositional environments for the different facies defined in the sediment sequence

Facies	Sedimentology		Geochemical composition	Depositional environment
Clastic facies				
1	*Blackish, banded carbonate clayey silt:*Clay-rich matrix mainly composed of phyllosilicates and silty fraction composed of calcite, quartz, and dolomite. Minor amounts of feldspars, high-magnesium calcite (HMC) and gypsum. Frequent biogenic components comprising aggregates of amorphous lacustrine organic matter, macrophyte remains and diatoms		TOC = 2.25–7.40%, TN = 0.25–0.70%, TOC/TN = 6.90–11.2, TS = 0.95–2.30%	Deep, monomictic, freshwater lake
2	*Grey, banded to laminated calcareous silts*: Calcite, quartz and dolomite silt-sized particles embedded in a clay-rich matrix. Minor amounts of feldspars, HMC, pyrite and gypsum. Presence of biogenic components: diatoms, amorphous lacustrine organic matter and land-derived plant remains (frequent)	Subfacies 2.1: dm-thick, laminated to banded intervals with regular, sharp contacts (Fig. 6.A.I)	TOC = 0.8–4.20%, TN = 0.10–0.45%, TOC/TN = 6.15–15.5, TS = 1.15–12.9%	Deep, monomictic, freshwater lake
		Subfacies 2.2: cm to mm-thick laminae with diffuse and irregular contacts intercalated within other facies (Fig. 6.A.II)		
3	*Black, massive to faintly laminated silty clay*: Clay-rich matrix dominant, with silt-sized calcite and quartz particles and frequent amorphous lacustrine organic matter aggregates. Minor amounts of dolomite, feldspars, HMC and gypsum		TOC = 0.95–2.10%, TN = 0.10–0.2%, TOC/TN = 7.40–10.5, TS = 0.40–1.00%	Deep, meromictic freshwater lake
6	*Grey and mottled, massive carbonate silt with plant remains and gypsum*: Sediments are composed of calcite followed by clay minerals, dolomite and quartz and minor amounts of HMC and gypsum nodules. Mottling and edaphic features are common. Abundant gastropods and large mm to cm-size terrestrial organic remains		TOC = 1.05–2.70%, TN = 0.10–0.20%, TOC/TN = 6.2–13.6%, TS = 1.40–11.5%	Ephemeral lake
Organogenic facies				
4	*Brown laminated sapropel with gypsum laminae and nodules*: Organic sediments are composed of amorphous algal matter, diatoms and some macrophyte remains, with minor amounts of clay minerals, calcite, dolomite and quartz. Gypsum laminae are composed of idiomorph, well-developed crystals ranging from 25 to 50 μm; mm to 1 cm-sized nodules also occur within the sediment (Fig. 6.A.II)		TOC = 0.90–24.3%, TN = 0.05–1.95%, TOC/TN = 5.35–25.45, TS = 2.15–31.0%	Saline water lake
5	*Variegated finely laminated carbonate mud and sapropel*: Sets of yellowish mm-thick laminae (authigenic carbonates (calcite, aragonite, dolomite)), dark-brown laminae (lacustrine organic matter, diatoms) and occasional grey carbonate silt laminae		TOC = 5.35–21.5%, TN = 0.50–1.75%, TOC/TN = 9.05–21.5, TS = 4.25–20.50%	Brackish water lake

low values, ranging from 1.7% to 4.4% (Fig. 7, Table 3). Minor TOC (%) variations have been observed within clastic dominant intervals, especially throughout the uppermost part of the sequence, due to the presence of layers with more abundant plant remains. TN values range from 0% to 2%, showing an analogue pattern as TOC. Relatively low TOC/TN ratios (generally below 10) indicate that most organic matter is authochthonous produced by freshwater algae (Meyers and Lallier-Vergès, 1999; Meyers, 2003).

TS curve parallels gypsum content, confirming the low content of sulphides (less than 5%) throughout the sediment sequence as observed after the XRD analyses. Values remain low (less than 3%) in clastic units, and reach up to 20% (12–20% on average) in organogenic-dominant units (Fig. 7).

Downcore variations in biogenic silica (BGS) mirror diatom concentration. They primarily reflect changes in primary productivity as delivered by diatoms in the euphotic zone (Colman et al., 1995; Johnson et al., 2001). However, due to moderate-to-low opal content we assume that the diatom signal has been influenced by dissolution. BGS values in core 1A–1K range between 0.5% and 12%. BGS remains low (between 0% and 2%) through the sediment sequence and only 5 major peaks (up to 12%) have been identified (Fig. 7). Although BGS shows no clear correlation with facies distribution, it is noticeable that maximum values are generally reached in organogenic facies whereas minimum values are reached in clastic intervals. Lake productivity is expected to be higher at those intervals characterized by higher nitrogen content and lower TOC/TN ratios (Meyers and Lallier-Vergès,

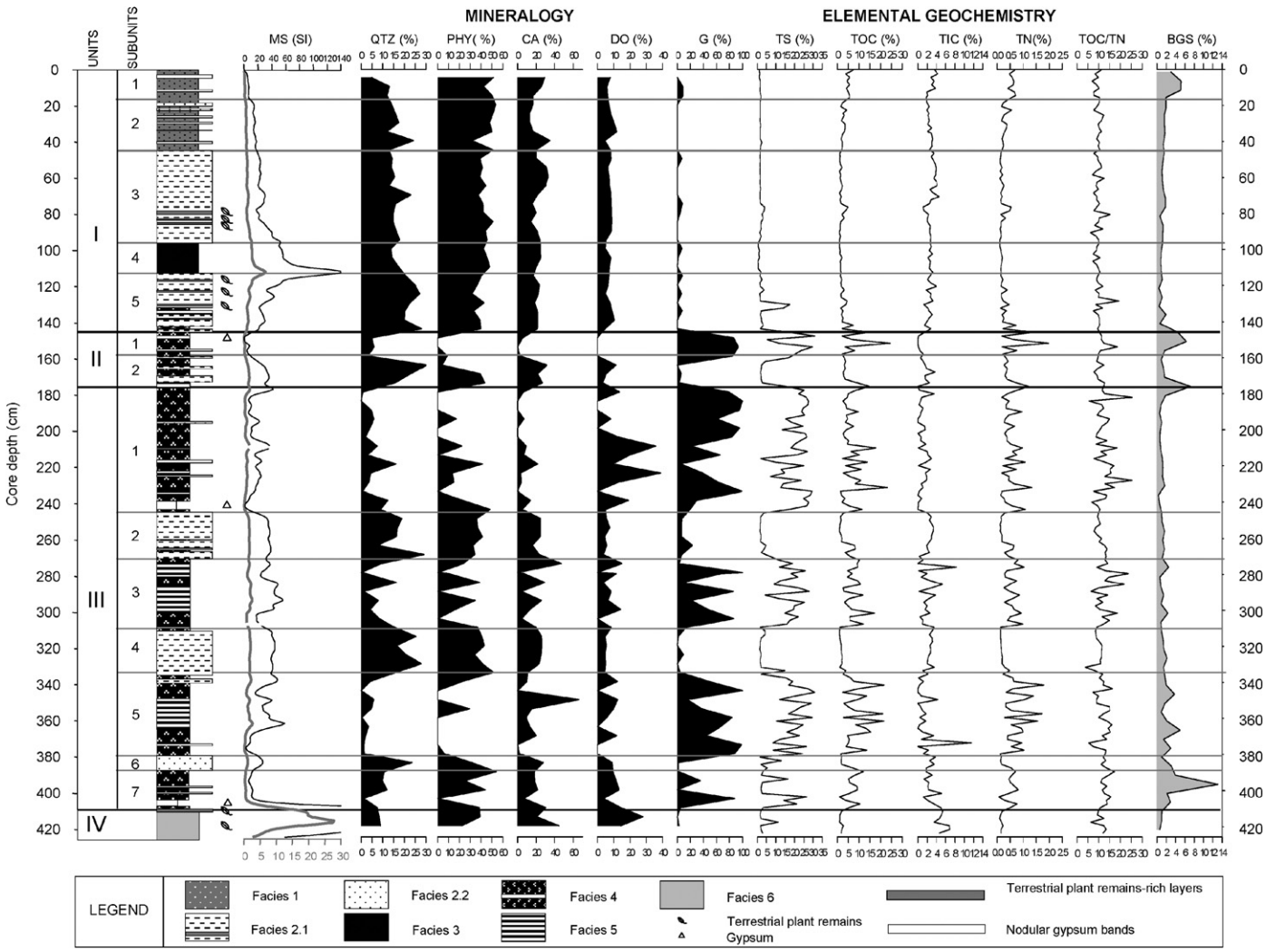

Fig. 7. Sedimentological (facies lithological units and Subunits) magnetic susceptibility, mineralogical and geochemical profiles of Core 1A–1K. QTZ: quartz; PHY: phylosilicates; CA: calcite; DO: dolomite; G: gypsum; TS: total sulphur; TOC: total organic carbon; TIC: total inorganic carbon; TN: total nitrogen; BGS: biogenic silica. A detailed facies legend is shown.

1999; Meyers, 2003). However the uppermost part of unit I (Subunit I.1), mainly composed of facies 1, also presents relatively high BGS content (Fig. 7). This latter increase in lake productivity could be related to lake eutrophication as a result of the development of agriculture in the region (Riera et al., 2004).

5. Discussion

According to facies distribution and mineralogical and geochemical composition, four main sedimentary units have been identified and correlated among all the cores in both sub-basins (Fig. 3). Several Subunits have been defined within these main units for core 1A–1K and they can be also identified in core 3A–1K (both cores in southeastern sub-basin). A short core with the sediment–water interface undisturbed was correlated with core 1A–1K to allow the reconstruction of upper 22 cm of the sequence, missed in core 1A–1K (Fig. 4). The main characteristics of the units are summarised in Fig. 5.

Sedimentary facies provide evidences of changes in lake level, organic productivity, oxic/anoxic conditions at the bottom of the lake, allogenic input and chemical concentration of the waters. Accordingly, the interpretation of facies in terms of lake level has allowed reconstruction of the variation of the Estanya lake level during the Holocene (Fig. 8). The use of paleosalinity as a proxy for changes in lake level, represented here by the percentage of TS, is based on the assumption that salinity varies inversely with depth, and water chemical concentration is controlled by changes in input (precipitation and groundwater) and evaporation regimes (Street-Perrott and Harrison, 1985).

Since sulphide content is below 5% according to XRD analyses as stated above, TS is assumed to represent gypsum content. This assumption has been applied in saline lake records with high sulphate content from Iberian

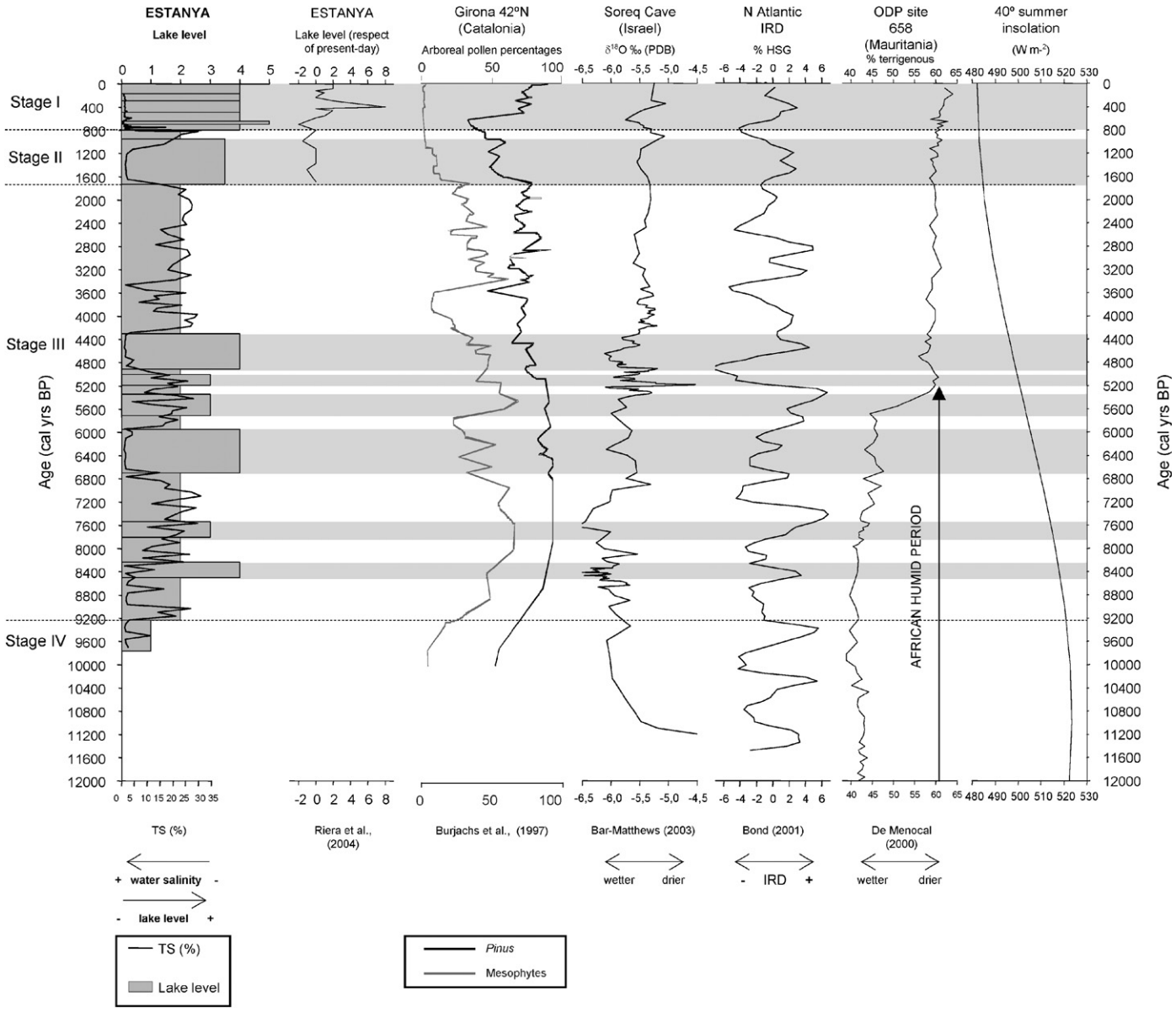

Fig. 8. Lake level reconstruction from the Estanya lake record during the Holocene compared with other paleorecords. From left to right: Lake level changes in Estanya from 2000 cal yr BP to the present (Riera et al., 2004); *Pinus* and Mesophytes content in Girona pollen sequence (Catalonia, NE Spain) (Burjachs et al., 1997); $\delta^{18}O$ per mil in Soreq Cave speleothem record (Israel) (Bar-Matthews et al., 2003); percentage of hematite stained grains (HSG) from ice rafted debris (IRD) record in N Atlantic (Bond et al., 2001); percentage of terrigenous sediments in ODP site 658 (offshore Mauritania) (De Menocal et al., 2000); and 40° summer insolation (in W m^{-2}). In Lake Estanya reconstruction horizontal bars represent estimated lake-level (from 1 to 5) for each sedimentary Subunit according to facies interpretation. (*Lake level*: 1: Ephemeral lake; 2: Saline lake; 3: Brackish lake; 3.5: Brackish to freshwater lake transition; 4: Freshwater lake; 5: Meromictic freshwater lake). Total sulphur (TS) percentage curve is represented as a paleosalinity proxy showing inverse relationship with estimated lake level.

Peninsula (Valero-Garcés et al., 2000a; Santisteban et al., 2004; Domínguez-Castro et al., 2006) and elsewhere (p.e. Hillesheim et al., 2005). Textural observations of both thin sections and SEM photographs (Fig. 6) clearly show that gypsum is authigenic and precipitates either in the water column or within the sediment. Authigenic gypsum deposits have been interpreted as indicative of high salinity episodes caused by a fall in water level in different lake records of Iberian Peninsula (Giralt et al., 1999; Schütt, 2000; Pérez et al., 2002; Rodó et al., 2002; Riera et al., 2004; González-Sampériz et al., in press). A common feature of these gypsum deposits is its association to organic matter (Schreiber and Tabakh, 2000) (Table 3), here represented by the simultaneous occurrence of TOC and TS peaks through the record (Fig. 7).

In Estanya, although the hydrological and hydrochemical balance of the lake is unknown, qualitative observations show a rapid response of lake level to precipitation and groundwater input during the last decades (Fig. 2). Assuming relatively constant compositional characteristic

of the aquifer waters, and absence of changes in aquifer structure during the Holocene, a direct relationship is recognised between increased water chemical concentration and deposition of saline facies and decreasing lake levels (Fig. 5).

Based on the environmental interpretation of the sedimentary facies, the mineralogy and the main compositional and geochemical proxies, four main depositional and hydrological stages, corresponding to the four main sedimentary units previously defined, are interpreted from the Estanya sedimentary sequence (Fig. 8).

5.1. Stage IV (425.5–409.5 cm, 9765–9230 cal BP): shallow, ephemeral lake

Although the early Holocene abrupt increase in effective moisture is a well-established feature of Holocene paleohydrology and climate variability in the Mediterranean regions (Roberts et al., 2004), the timing, duration and intensity of this humid period show a large regional variability. Regional syntheses of lake-level data for the Western Mediterranean, with a limited dataset of the Iberian Peninsula (Harrison and Digerfeldt, 1993; Harrison et al., 1996) show similar complexity. The Early Holocene in Atlantic-Iberia and the central Pyrenees was moist and warm (Montserrat, 1992; Allen et al., 1996; González-Sampériz et al., 2006), with semi-arid extreme continental conditions and higher lake levels than today in the Ebro Basin (Davis, 1994; González-Sampériz et al., in press), and also with moister conditions in northern and southern Mediterranean areas, as Banyoles and Salines lakes, respectively (Pérez-Obiol and Julià, 1994; Roca and Julià, 1997; Julià et al., 1998; Wansard et al., 1998). The early Holocene corresponds to the most humid period in some records from southeastern Spain (Julià et al., 1994; Giralt et al., 1999). Nevertheless there are other southern sequences as Laguna Medina in Cádiz (Reed et al., 2001), Siles and Ojos de Villaverde in Segura Mountains (Carrión, 2002) and Sierra de Gádor (Carrión et al., 2003), where the highest lake level and the maximum development of mesophytes indicates that the most humid period in the region corresponds to the Mid-Holocene.

The Estanya record fits with most Mediterranean (Ariztegui et al., 2000), regional (de Menocal et al., 2000) and global (Mayewski et al., 2004) paleorecords and clearly shows the dramatic increase in water availability in the region after 9.2 ka.

5.2. Stage III (409.5–176 cm, 9230–1730 cal BP): fluctuating saline to brackish lake with centennial-scale fresher periods

A 1 cm thick, black massive sandy layer with abundant land-derived organic matter over an erosive surface constitutes the base of the sequence and marks a rapid lake transgression and the onset of the Holocene more humid conditions at 9.2 ka. This abrupt change has been clearly recorded through the whole basin (Fig. 3) showing a small chronological mismatch between the two sub-basins, likely due to dating uncertainities. During the Early and Mid Holocene (9.2–4.2 ka.), Lake Estanya was a permanent lake, with fluctuating saline to brackish and to freshwater conditions. These oscillations represent millennial scale humid and arid cycles. According to the chronological model available, three century-long periods of increased run-off and sediment delivery and less saline conditions occurred at 8.5–8.2, 6.7–5.9, and 4.9–4.2 ka.

5.2.1. The Early Holocene

A number of small floods occurred before the large event represented by Subunit III.6 (8500–8230 cal BP). Several factors are conducive to increased clastic input in a permanent saline lake as Estanya, but likely a combination of increased run-off and a change in the vegetation cover in the watershed played a significant role. Lake waters were still saline after the period of more intense floods as indicated by the presence of mm-thick gypsum-rich laminae.

The occurrence of laminated, authigenic carbonate-rich facies 5 after 8.2 ka marks a change in the lake environment. Thus, Subunit III.5 (8230–6700 cal BP) is characterized by the alternation of periods of higher salinity (facies 4: gypsum laminae and algal mat development) and lower salinity (facies 5: carbonate laminae and algal mats), with more frequent periods of increased clastic input, and periods of meromixis (finely laminated facies). Some mm to cm-thick layers of facies 2.2 also occur, especially at the upper part indicating a transition to a period with relatively high lake levels, with the lake system dominated by clastic-influenced depositional environments and some fluctuations in salinity towards brackish conditions (Subunit III.4: 6700–5940 cal BP). Intermediate lake levels with frequent periods of increased clastic input characterize this period (8.2–5.9 cal ka) in Estanya (Fig. 8). Pollen records in Mediterranean regions from Spain show the maximum development of temperate taxa during this time interval (Burjachs et al., 1997). At a regional scale, this period correspond to the development of the S1 sapropel in the Mediterranean Sea (Ariztegui et al. 2000) and the African humid period (de Menocal, 2001) (Fig. 8).

5.2.2. The transition to the Mid Holocene

Brackish environments with calcite formation in the epilimnion and anoxic bottom conditions dominate the period 5.9–4.9 ka (Subunit III.3, 5940–4910 cal BP) with some minor gypsum-rich periods. Clastic, laminated facies 2.1 composed of cm-thick fining upward sequences of darker coarse and finer grey facies dominate again during the period 4.9–4.2 ka (Subunit III.2 4910–4250 cal BP) marking another period of fresher lake waters, increased runoff and sediment delivery to the lake. In Estanya, decreasing flooding events after 4.2 ka led to the deposition of carbonate facies 5 that progressively were substituted by gypsum-rich facies 4 (Subunit 1 (4250–1730 cal BP))

indicative of saline environments, lower lake level and reduced run-off and sediment supply.

Evidence for an overall decrease in moisture availability during the second part of the Mid Holocene in the Iberian Peninsula comes from lake records (Pons and Reille, 1988; Davis, 1994; Pérez-Obiol and Julià, 1994; Van der Knaap and Van Leeuwen, 1995; Yll et al., 1997; Reed et al., 2001; Carrión et al., 2003; González-Sampériz, et al., in press) and also fluvial records, with increase in alluvial overbank deposits, perhaps due to increased sediment mobility related to the drier climate (Benito et al., 1996). Evidences for this arid episode elsewhere in the Mediterranean are also widespread in lakes (Roberts et al., 2001b; Sadori and Narcisi, 2001; Magny et al., 2002; Magny, 2004), rivers (Macklin et al, 2006), speleothems (Bar-Matthews et al., 2003; Drysdale et al., 2006) and marine records (Ariztegui et al., 2000). This arid episode also coincides with the end of the African Humid Period (de Menocal et al., 2000) (Fig. 8). The onset of arid conditions in Estanya occurs after 4250 cal yr BP and coincides with most of the above-mentioned records, considering the uncertainties of the chronological model.

5.3. Stage II (176–146 cm, 1730–795 cal BP): increased clastic input, intermediate, fluctuating lake level

A long episode of higher clastic input occurred after the Roman Age and during the Visigothic and Muslim periods (1730–950 cal BP) when brackish and saline environments (organic facies 5 and some facies 4) dominated in the Estanya lake (Fig. 8).

This stage correlates with a period of relatively higher lake levels, undisturbed mixed woodland and restricted farming practices during Visigothic times (Riera et al., 2004), followed by high charcoal concentrations and pollen assemblages changes indicative of the first phase of large-scale deforestation during the 1200–1000 cal BP period. However, our reconstruction show increased clastic input in the central areas of the lake occurred from 1800 to 1000 cal BP, prior to the large deforestation interpreted by Riera et al. (2004). It is consequently more likely that this change in sediment supply to the inner areas of the lake was caused by an increase in run-off due to climate change.

Increased erosion in the watershed at about 1.7 ka is unlikely caused by human disturbance and deforestation because historical and archaeological records show a low impact of the population after Roman times in the Estanya area and pollen assemblages show undisturbed mixed woodland landscape for this time (Riera et al., 2004). However, the increase in sedimentation rate after 650 cal yrs. BP is most likely cause by intense deforestation after the Christian conquest of the area. An erosion model of the Estanya catchment indicates that erosion rates are strongly dependant on the vegetation cover and soil type, and they are much higher in cultivated areas (López-Vicente et al., 2005).

Both littoral (Riera et al, 2004) and offshore cores show evidences for a dry period during the 950–800 cal BP period. Decreasing MS values and clastic input and deposition of massive to barely laminated facies 4 with abundant gypsum nodules reflects a lower flood frequency, shallower lake levels and more concentrated waters during the period 950–800 cal BP. Arid periods have also been reported at this time from Iberian Range lakes (La Cruz Lake, Julià et al., 1998) and northern Africa (Lamb et al., 1995).

From a hydrological point of view, the last 1.7 ka show higher lake levels than before, with a short dry period from 950–800 cal BP. This increase in moisture availability was also documented by Lamb et al (1995) in Tigalmamine (Morocco).

5.4. Stage I (in core 1A–1K: 146–0 cm, in short core: 70–0 cm; 795 cal BP—modern): relatively high lake level, fluctuating salinity, high clastic input

The onset of this stage at about 795 cal yrs BP represents a large change in the limnology of the lake, characterized by relatively higher lake levels, low chemical concentrations and high detrital input pointing to high erosion rates in the watershed. Quartz and clay mineral contents are the highest in the core. Sedimentary facies and MS values define two fining upward sequences. The first one from 795–640 cal BP (Subunits I.5 and I.4) is characterized by an increasing trend in MS, decreasing in quartz and increasing in clay minerals. The top one (640 cal yrs BP to present, Subunits 3–1) shows decreasing MS and quartz and higher clay mineral content in the upper part (Fig. 7). Higher clay content and lower quartz content in this sequence can be explained as a reflection of similar erosion rates as before, but higher lake levels, that make more difficult for coarse sediments to reach the centre of the lake.

In the littoral core described by Riera et al (2004), a rise in water level is also indicated for the period 880–730 cal BP corresponding to the onset of deposition of unit I in the off-shore core (Fig. 8). This period correspond with the expansion of human settlements in the region after the Christian conquest in 1075 AD (880 cal yr BP), the increase in farming practices and the construction of agricultural terraces (Palet and Riera, 1994; Riera et al., 2004).

Although there is a clear human influence on the lake during this stage (i.e., farming practices, artificial water management) and several canals were constructed 800 cal yr BP, as documented by previous studies (Riera et al., 2004, 2006), not all the environmental changes recorded during this stage can be attributed to human activities. In addition, as mentioned above, present-day observations show that lake level changes primarily respond to changes in precipitations (Fig. 2).

In our core, the period ca. 695–640 cal BP, is characterized by the unique occurrence of fine-grained, black, sulphide-bearing facies 3 with thin facies 2.2 laminae with diffuse boundaries that suggest permanent, meromictic

conditions in the lake. Since there is no indication of increased salinity as a possible factor to cause permanent water stratification, it is more likely that a period of higher lake levels was conducive to water stratification and stagnation, more pronounced in the deeper southern sub-basin. This period corresponds to the second part of the Medieval Warm Period extending from 735 to 605 cal BP (Stine, 1994, 1998; Lamb et al., 1995).

At about 640 cal BP, deposition of relatively coarser facies 2 marks the onset of another period of increased sediment delivery that would until till 490 cal yrs BP. This period (Subunit I.3, 640–490 cal BP), although dominated by banded, clastic facies 2.1, contains thin intervals of laminated carbonate-rich facies 5 and gypsum-rich facies 5 indicating rapid changes in the limnological conditions. After 490 cal yrs BP, finer sediments of facies 1 dominate indicating higher lake levels and freshwater conditions (Subunit I.2, 490–295 cal BP). The last 300-year period in Estanya (Subunit I.1, 295 cal BP—modern) shows a relative decrease in quartz content and MS values suggest decrease clastic input from the watershed (Fig. 7). The increase in calcite could be explained by an increase in endogenic calcite production in the lake, coherent with the increase in TOC, TN and BGS in this unit.

The reconstructed environmental and hydrological evolution for the last 2000 years from the littoral core shows a similar trend of fluctuating but relatively higher lake levels than before (Riera et al., 2004), but also some differences that could indicate different sensitivity of littoral versus off-shore environments to climate and environmental change and also reflect the chronological uncertainties of both age models. Two periods of low lake level occurred in the littoral core between 1135–880 and 735–605 cal BP. The first one could correlate with the top of Subunit II.1 in the offshore core. The second one, considered as the driest during the last 2000 years, is assigned to the MWP. The highest humidity in the littoral zone is interpreted for the period 605–375 cal BP, and a second humid phase for 205–60 cal BP corresponding to the LIA. In the offshore core, alternating facies indicate many fluctuations during the last centuries, but the deepest facies seems to correspond to Subunit I.3 (755–605 cal BP). This fits with the overall trend across the Mediterranean basin showing maximum wetness around 705–555 cal yr BP overlapping with the second half of the European Medieval Warm Period (Mayewski et al., 2004; Roberts et al., 2004). This period corresponds to another RCC at 600 cal BP that continues until 150 cal yrs BP and it is characterized by glacier advance, strengthened westerlies in the Northern Hemisphere and humid conditions in equatorial Africa (Verschuren et al., 2000). A more detailed dating is needed to resolve these inconsistencies. In any case, all available records point to increased climate variability and hydrological fluctuations in Spain during the last centuries prior and during the Little Ice Age similar to those documented in the upper part of the Estanya sequence.

6. Conclusions

The presence of humid and arid periods of different intensity and extent, at different timescales recorded at Estanya, underlines the complexity and singularity of the Iberian Peninsula hydrological evolution during the Holocene. The Estanya record shows a large increase in water availability after 9.2 ka, fluctuating lake levels and salinity during the period 9.2–4.2 ka; periods of increased run-off and sediment delivery and less saline conditions occurred at 8.5–8.2, 6.7–5.9, and 4.9–4.2 ka. Dominant lower lake levels and concentrated waters during the period 4.2–0.8 ka were punctuated by a higher lake level, higher clastic input episode ca. 1.7–1 ka. Fluctuating, but higher lake levels occurred during the last 800 years.

Comparison of the main hydrological phases in Lake Estanya with Western Mediterranean and North Atlantic records provides some insights in the spatial and temporal extent of these episodes. The Estanya record documents generally higher lake levels and effective moisture during the early Holocene, and a decreasing trend during the Mid Holocene, comparable to most Mediterranean paleoclimate reconstructions. However, our results clearly show a significant increase in water availability during the last 2000 years, similar to other examples in northern Africa.

Acknowledgements

Financial support for research at Lake Estanya was provided by the Spanish Inter-Ministry Commission of Science and Technology (CICYT), through the projects LIMNOCLIBER (REN2003-09130-C02-02) and IBER-LIMNO (CGL2005-20236-E/CLI). *Instituto de Estudios Altoaragoneses* (IEA) also provided financial support for in-situ measurements and radiocarbon dating. CONAI+D–Obra Social CAJA INMACULADA partially funded DRX and SEM analyses in University of Cádiz by means of a travel grant (*Programa Europa*).

M. Morellón is supported by a Ph.D. fellowship funded by the CONAI+D (Aragonese Regional Government) and A. Moreno holds a Marie Curie programme post-doctoral fellowship.

We are grateful to Doug Schnurrenberger, Anders Noren and Mark Shapley (LRC, University of Minnesota) for the 2004 coring expedition. Daniel Ariztegui (University of Geneva) and Michael Schnelmann (Geological Institute—ETH Zürich) performed the seismic survey of the lake-basin in 2002. Miguel Ángel García Vera (Ebro Basin Watershed Authority (CHE)) and Spanish National Meteorological Institute (INM) provided climatological data from Santa Ana Reservoir. Nitrogen analyses were performed by Elena Lahoz (IPE-CSIC) and water chemistry analyses were performed by Teresa López and Maribel Poc (EEAD-CSIC). Manuel López-Vicente (EEAD-CSIC) provided useful information about the catchment geomorphology. Achim Brauer (GFZ-Postdam) supervised thin section preparation and Celia Martín

(University of Cádiz) performed thin section photographs and preliminary observations. We thank anonymous reviewers for their helpful comments and their criticism, which led to a considerable improvement of the manuscript.

References

Allen, J.R., Huntley, B., Watts, W.A., 1996. The vegetation and climate of northwest Iberia over the last 14000 yr. Journal of Quaternary Science 11, 125–147.

Anker, S.A., Colhoun, E.A., Barton, C.E., Peterson, M., Barbetti, M., 2001. Holocene vegetation and paleoclimatic and paleomagnetic history from Lake Johston, Tasmania. Quaternary Research 56, 264–274.

Ariztegui, D., Asioli, A., Lowe, J.J., Trincardi, F., Vigliotti, L., Tamburini, F., Chondrogianni, C., Accorsi, C.A., Bandini Mazzanti, M., Mercuri, A.M., Van der Kaars, S., McKenzie, J.A., Oldfield, F., 2000. Palaeoclimate and the formation of sapropel S1: inferences from Late Quaternary lacustrine and marine sequences in the central Mediterranean region. Palaeogeography, Palaeoclimatology, Palaeoecology 158, 215–240.

Ávila, A., Burrel, J.L., Domingo, A., Fernández, E., Godall, J., Llopart, J.M., 1984. Limnología del Lago Grande de Estanya (Huesca). Oecologia Aquatica 7, 3–24.

Bar-Matthews, M., Ayalon, A., Gilmour, M., Matthews, A., Hawkesworth, C.J., 2003. Sea-land oxygen isotopic relationship from planktonic foraminifera and speleothems in the Eastern Mediterranean region and their implication for paleorainfall during interglacial interval. Geochimica et Cosmochimica Acta 67, 3181–3199.

Benito, G., Machado, M.J., Pérez-González, A., 1996. Climate change and flood sensitivity in Spain. In: Branson, J., Brown, A.G., Gregory, K.J. (Eds.), Global Continental Changes: The Context of Palaeohydrology, vol. 115. Special Publication-Geological Society of London, pp. 85–98.

Bond, G., Showers, W., Cheseby, M., Lotti, R., Almasi, P., de Menocal, P., Priore, P., Cullen, H., Hajdas, I., Bonani, G., 1997. A pervasive millennial-scale cycle in North Atlantic Holocene and Glacial climates. Science 278, 1257–1266.

Bond, G., Kromer, B., Beer, J., Muscheler, R., Evans, M.N., Showers, W., Hoffman, S., Lotti-Bond, R., Hajdas, I., Bonani, G., 2001. Persistent solar influence on North Atlantic climate during the Holocene. Science 294, 2130–2136.

Brauer, A., Mingram, J., Frank, U., Günter, C., Schettler, G., Wulf, S., Zolitschka, B., Negendank, J.F.W., 2000. Abrupt environmental oscillations during the Early Weichselian recorded at Lago Grande di Monticchio, southern Italy. Quaternary International 73–74, 79–90.

Burjachs, F., Giralt, S., Roca, J.R., Seret, G., Julià, R., 1997. Palinología holocénica y desrtización en el Mediteráneo occidental. In: Ibáñez, J.L., Valero-Garcés, B., Machado, C. (Eds.), El paisaje Mediterráneo a través del tiempo y del espacio. Implicaciones en la desertificación. Geoforma ediciones, Logroño, pp. 379–394.

Carrión, J.S., 2002. Patterns and processes of Late Quaternary environmental change in a montane region of southwestern Europe. Quaternary Science Reviews 21, 2047–2066.

Carrión, J.S., Sánchez-Gómez, P., Mota, J.F., Yll, R., Chaín, C., 2003. Holocene vegetation dynamics, fire and grazing in the Sierra de Gádor, southern Spain. The Holocene 13, 839–849.

Chung, F.H., 1974a. Quantitative interpretation of X-ray diffraction patterns of mixtures I. Matrix-flushing method for quantitative multicomponent analysis. Journal of Applied Crystallography 7, 519–525.

Chung, F.H., 1974b. Quantitative interpretation of X-ray diffraction patterns of mixtures. II. Adiabatic principle of X-ray diffraction analysis of mixtures. Journal of Applied Crystallography 7, 526–531.

Colman, S.M., Peck, J.A., Karabanov, E.B., Carter, S.J., Bradbury, J.P., King, J.W., Williams, D.F., 1995. Continental climate response to orbital forcing from biogenic silica records in Lake Baikal. Nature 378, 769–771.

Davis, B.A.S., 1994. Paleolimnology and Holocene environmental change from endorheic lakes in the Ebro Basin, north-east Spain. Ph.D. Thesis, University of Newcastle upon Tyne, 317p.

Davis, B., Stevenson, T., Juggins, S., Brewer, S., 2001. Short-term climate events in the Mediterranean area during the Holocene: some preliminary results using pollen based reconstructions. Terra Nostra 2, 24–29.

De Master, D.J., 1981. The supply and accumulation of silica in the marine environment. Geochimica et cosmochimica Acta 32, 1128–1140.

De Menocal, P., Ortiz, J., Guilderson, T., Sarnthein, M., 2000. Coherent high-and-low-latitude climate variability during the Holocene Warm Period. Science 288, 2198–2202.

Domínguez-Castro, F., Santisteban, J.I., Mediavilla, R., Dean, W.E., López-Pamo, E., Gil-García, M.J., Ruiz-Zapata, M.B., 2006. Environmental and geochemical record of human-induced changes in C storage during the last millennium in a temperate wetland (Las Tablas de Daimiel National Park, central Spain). Tellus B 58, 573–585.

Drysdale, R., Zanchetta, G., Hellstrom, J., Maas, R., Fallick, A., Pickett, M., Cartwright, I., Piccini, L., 2006. Late Holocene drought responsible for the collapse of Old World civilizations is recorded in an Italian cave flowstone. Geology 34, 101–104.

Duplessy, J.-C., Cortijo, E., Kallel, N., 2005. Marine records of Holocene climatic variations. Comptes Rendus Geosciences 337, 87–95.

García-Herrera, R., Gimeno, L., Ribera, P., Hernández, E., 2005. New records of Atlantic hurricanes from Spanish documentary sources. Journal of Geophysical Research 110, D03109.

García-Vera, 2004. Estudio hidrogeológico del Sinclinal de Estopiñán (Huesca) y de la Riera de Vall-Major (Lleida). Asistencia técnica. Fundación Centro Internacional de Hidrología Subterránea. Confederación Hidrográfica del Ebro (unpublished) 130p.

Gasse, F., 2000. Hydrological changes in the African tropics since the Last Glacial Maximum. Quaternary Science Reviews 19, 189–211.

Giralt, S., Burjachs, F., Roca, J.R., Julià, R., 1999. Late Glacial to Early Holocene environmental adjustment in the Mediterranean semi-arid zone of the Salines playa-lake (Alacante, Spain). Journal of Paleolimnology 21, 449–460.

González-Sampériz, P., Valero-Garcés, B.L., Moreno, A., Jalut, G., García-Ruiz, J.M., Martí-Bono, C., Delgado-Huertas, A., Navas, A., Otto, T., Dedoubat, J.J., 2006. Climate variability in the Spanish Pyrenees during the last 30,000 yr revealed by the El Portalet sequence. Quaternary Research 66, 38–52.

González-Sampériz, P., Valero-Garcés, B.L., Moreno, A., Morellón, M., Navas, A., Machín, J., Delgado-Huertas, A., in press. Vegetation changes and hydrological fluctuations in the Central Ebro Basin (NE Spain) since the Late Glacial period: saline lake records. Paleogeography, Palaeoclimatology, Palaeoecology.

Harrison, S.P., Digerfeldt, G., 1993. European lakes as palaeohydrological and palaeoclimatic indicators. Quaternary Science Reviews 12, 233–248.

Harrison, S.P., Yu, G., Tarasov, P.E., 1996. Late Quaternary lake-level record from northern Eurasia. Quaternary Research 45, 138–159.

Hillesheim, M.B., Hodell, D.A., Leyden, B.W., Brenner, M., Curtis, J.H., Anselmetti, F.S., Ariztegui, D., Buck, D.G., Guilderson, T.P., Rosenmeier, M.F., Schnurrenberger, D.W., 2005. Climate change in lowland Central America during the Late Deglacial and Early Holocene. Journal of Quaternary Science 20, 363–376.

Hu, H., Neelin, J.D., 2005. Dynamical mechanisms for African monsoon changes during the Mid-Holocene. Journal of Geophysical Research 110.

Hurrell, J.W., 1995. Decadal trends in the North Atlantic Oscillation: regional temperatures and precipitation. Science 269, 676–679.

IGME, 1982. Mapa Geológico de España, 1:50.000. No. 289. Benabarre. Instituto Geológico y Minero, Madrid.

Jalut, G., Amat, A.E., Bonnet, L., Gauquelin, T., Fontugne, M., 2000. Holocene climatic changes in the Western Mediterranean, from

south-east France to south-east Spain. Paleogeography, Palaeoclimatology, Palaeoecology 160, 255–290.

Johnson, T.C., Barry, S.L., Chan, Y., Wilkinson, 2001. Decadal record of climate variability spanning the past 700 yr in the Southern Tropics of East Africa. Geology 29 (1), 83–86.

Julià, R., Negendank, J.F.W., Seret, G., Brauer, A., Burjachs, F., Endres, C., Giralt, S., Parés, J.M., Roca, J.R., 1994. Holocene climatic change and desertification in the Western Mediterranean region. Terra Nostra 1, 81–84.

Julià, R., Burjachs, F., Dasí, M.J., Mezquita, F., Miracle, M.R., Roca, J.R., Seret, G., Vicente, E., 1998. Meromixis origin and recent trophic evolution in the Spanish mountain lake La Cruz. Aquatic Sciences 60 (4), 279–299.

Lamb, H.F., Gasse, F., Benkaddour, A., El Hamouti, N., van der Kaars, S., Perkins, W.T., Pearce, N.J., Roberts, C.N., 1995. Relation between century-scale Holocene arid intervals in tropical and temperate zones. Nature 373, 134–137.

León-Llamazares, A., 1991. Caracterización agroclimática de la provincia de Huesca. MAPA, Madrid.

Liu, Z., Wang, Y., Gallimore, R., Notaro, M., Prentice, I.C., 2006. On the cause of abrupt vegetation collapse in North Africa during the Holocene: climate variability vs. vegetation feedback. Geophysical Research Letters 33 (22), L22709.

López-Vicente, M., Nelson, R., Stockle, C.O., Navas, A., Machín, J., 2005. Modelización de la capacidad de transporte distribuida en subcuencas endorreicas del Pirineo oscense. In: Proceedings of the II Simposio Nacional Sobre Control de la Degradación de Suelos, Madrid, Spain.

Luque Marín, J.A., 2003. El lago de Sanabria: un sensor de las oscilaciones climáticas del Atlántico Norte durante los últimos 6.000 años. Unpublished Ph.D. Thesis. University of Barcelona. Barcelona, Spain.

Macklin, M.G., Benito, G., Gregory, K.J., Johnstone, E., Lewin, J., Michczynska, D.J., Soja, R., Starkel, L., Thorndycraft, V.R., 2006. Past hydrological events reflected in the Holocene fluvial record of Europe. Catena 66, 145–154.

Magny, M., 2004. Holocene climate variability as reflected by mid-European lake-level fluctuations and its probable impact on prehistoric human settlements. Quaternary International 113, 65–79.

Magny, M., Miramont, C., Sivan, O., 2002. Assessment of the impact of climate and anthropogenic factors on Holocene Mediterranean vegetation in Europe on the basis of palaeohydrological records. Paleogeography, Palaeoclimatology, Palaeoecology 186 (1–2), 47–59.

Mangili, C., Brauer, A., Moscariello, A., Naumann, R., 2005. Microfacies of detrital event layers deposited in Quaternary varved lake sediments of the Piànico-Sèllere Basin (northern Italy). Sedimentology 52, 927–943.

Martínez-Peña, M.B., Pocoví, A., 1984. Significado tectónico del peculiar relieve del Sinclinal de Estopiñán (Prepirineo de Huesca). In: Proceedings of the I Congreso Español de Geología, Segovia, Spain, vol. III, pp. 199–206.

Mayewski, P.A., Rohling, E.E., Stager, J.C., Karlén, W., Maasch, K.A., Meeker, L.D., Meyerson, E.A., Gasse, F., Kreveld, S.v., Holmgren, K., Lee-Thorp, J., Rosqvist, G., Rack, F., Staubwasser, M., Schneider, R.R., Steig, E.J., 2004. Holocene climate variability. Quaternary Research 62, 243–255.

Meyers, P.A., 2003. Applications of organic geochemistry to paleolimnological reconstructions: a summary of examples from the Laurentian Great Lakes. Organic Geochemistry 34, 261–289.

Meyers, P.A., Lallier-Vergès, E., 1999. Lacustrine sedimentary organic matter records of Late Quaternary paleoclimates. Journal of Paleolimnology 21, 345–372.

Montserrat, J., 1992. Evolución glaciar y postglaciar del clima y la vegetación en la vertiente sur del Pirineo: estudio palinológico. Monografías del Instituto Pirenaico de Ecología-CSIC, Zaragoza, 147p.

Müller, P.J., Schneider, R., 1993. An automated leaching method for the determination of opal in sediments and particulate matter. Deep-Sea Research I 40 (3), 425–444.

Muñoz-Díaz, D., Rodrigo, F.S., 2003. Effects of the North Atlantic Oscillation on the probability for climatic categories of local monthly rainfall in southern Spain. International Journal of Climatology 23, 381–397.

Palet, J.M., Riera, S., 1994. Landscape dynamics from Iberian-Roman (2nd-1st centuries BC) to early medieval times (12th century) in the Montjuïc-El Port sector (Plain of Barcelona, NE Iberian Peninsula). Archaeologica Madiaevalia 21, 517–540.

Peinado Lorca, M., Rivas-Martínez, S., 1987. La vegetación de España. Colección Aula abierta, 544p.

Peñalba, M.C., Arnold, M., Guiot, J., Duplessy, J.C., De Beaulieu, J.L., 1997. Termination of the Last Glaciation in the Iberian Peninsula inferred from the pollen sequence of Quintanar de la Sierra. Quaternary Research 48, 205–214.

Pérez, A., Luzón, A., Roc, A.C., Soria, A.R., Mayayo, M.J., Sánchez, J.A., 2002. Sedimentary facies distribution and genesis of a recent carbonate-rich saline lake: Gallocanta Lake, Iberian Chain, NE Spain. Sedimentary Geology 148, 185–202.

Pérez-Obiol, R., Julià, R., 1994. Climate change on the Iberian Peninsula recorded in a 30.000 yr pollen record from Lake Banyoles. Quaternary Research 41, 91–98.

Pons, A., Reille, M., 1988. The Holocene and upper Pleistocene pollen record from Padul (Granada, Spain): a new study. Palaeogeography, Palaeoclimatology, Palaeoecology 66, 243–263.

Reed, J.M., Stevenson, A.C., Juggins, S., 2001. A multi-proxy record of Holocene climatic change in southwestern Spain: the Laguna de Medina, Cádiz. The Holocene 11 (6), 707–719.

Reimer, P.J., Baillie, M.G.L., Bard, E., Bayliss, A., Beck, J.W., Bertrand, C.J.H., Blackwell, P.G., Buck, C.E., Burr, G.S., Cutler, K.B., Damon, P.E., Edwards, R.L., Fairbanks, R.G., Friedrich, M., Guilderson, T.P., Hogg, A.G., Hughen, K.A., Kromer, B., McCormac, G., Manning, S., Ramsey, C.B., Reimer, R.W., Remmele, S., Southon, J.R., Stuiver, M., Talamo, S., Taylor, F.W., van der Plicht, J., Weyhenmeyer, C.E., 2004. IntCal04 terrestrial radiocarbon age calibration, 0–26 Cal Kyr BP. Radiocarbon 46 (3), 1029–1058.

Riera, S., Wansard, R., Julià, R., 2004. 2000-year environmental history of a karstic lake in the Mediterranean Pre-Pyrenees: the Estanya lakes (Spain). Catena 55, 293–324.

Riera, S., Lopez-Saez, J.A., Julià, R., 2006. Lake responses to historical land use changes in northern Spain: the contribution of non-pollen palynomorphs in a multiproxy study. Review of Palaeobotany and Palynology 141 (1–2), 127–137.

Rivas-Martínez, S., 1982. Étages bioclimatiques, secteurs chorologiques et séries de végetation de l'Espagne méditerranéenne. Ecología Mediterranea VIII (1–2), 275–288.

Roberts, N., Meadows, M.E., Dodson, J.R., 2001a. The history of Mediterranean-type environments: climate, culture and landscape. The Holocene 11, 631–634.

Roberts, N., Reed, J.M., Leng, M.J., Kuzucuolu, C., Fontugne, M., Bertaux, J., Woldring, H., Bottema, S., Black, S., Hunt, E., Karabiyikoglu, M., 2001b. The tempo of Holocene climatic change in the eastern Mediterranean region: new high-resolution crater-lake sediment data from central Turkey. The Holocene 11, 719–734.

Roberts, C.N., Stevenson, T., Davis, B., Cheddadi, R., Brewster, S., Rosen, A., 2004. Holocene climate, environment and cultural change in the circum-Mediterranean region. In: Battarbee, R.W. (Ed.), Past Climate Variability through Europe and Africa, vol. 6. Springer, Dordrecht, pp. 343–362.

Roca, J.R., Julià, R., 1997. Late-Glacial and Holocene lacustrine evolution based on ostracode assemblages in southeastern Spain. Geobios 30 (6), 823–830.

Rodó, X., Giralt, S., Burjachs, F., Comín, F.A., Tenorio, R.G., Julià, R., 2002. High-resolution saline lake sediments as enhanced tools for relating proxy paleolake records to recent climatic data series. Sedimentary Geology 148, 203–220.

Sadori, L., Narcisi, B., 2001. The Postglacial record of environmental history from Lago di Pergusa, Sicily. The Holocene 11, 655–670.

Sancho Marcén, C., 1988a. Geomorfología de la Cuenca Baja del Río Cinca. Unpublished Ph.D. Thesis. University of Zaragoza. Zaragoza, Spain, 743p.

Sancho Marcén, C., 1988b. El Polje de Saganta (Sierras Exteriores pirenaicas, prov. de Huesca). Cuaternario y Geomorfología 2 (1–4), 107–113.

Santisteban, J.I., Mediavilla, R., López-Pamo, Dabrio, C.J., Ruiz-Zapata, M.B., Gil García, M.J., Castaño, S., Martínez-Alfaro, P.E., 2004. Loss on ignition: a qualitative or quantitative method for organic matter and carbonate mineral content in sediments? Journal of Paleolimnology 32, 287–299.

Schreiber, B.C., Tabakh, M.E., 2000. Deposition and early alteration of evaporites. Sedimentology 47, 215–238.

Schnurrenberger, D., Russell, J., Kelts, K., 2003. Classification of lacustrine sediments based on sedimentary components. Journal of Paleolimnology 29, 141–154.

Schütt, B., 2000. Holocene paleohydrology of playa lakes in northern and central Spain: a reconstruction based on the mineral composition of lacustrine sediments. Quaternary International 73/74, 7–27.

Stine, S., 1994. Extreme and persistent drought in California and Patagonia during medieval time. Nature 369, 546–549.

Stine, S., 1998. Medieval climatic anomaly in the Americas. In: Issar, A.S., Brown, N. (Eds.), Environment and Society in Times of Climatic Change. Kluwer, Dordrecht, pp. 43–67.

Street-Perrott, F.A., Harrison, S.P., 1985. Lake levels and climate reconstruction. In: Hecht, A. (Ed.), Paleoclimate Analysis and Modeling. Wiley, New York, pp. 291–340.

Trigo, R.M., Palutikof, J.P., 2001. Precipitation scenarios over Iberia: a comparison between direct GCM output and different downscaling techniques. Journal of Climate 14, 4442–4446.

Valero-Garcés, B., González-Sampériz, P., Delgado-Huertas, A., Navas, A., Machín, J., Kelts, K., 2000a. Late Glacial and Late Holocene environmental and vegetational change in Salada Mediana, central Ebro Basin, Spain. Quaternary International 73/74, 29–46.

Valero-Garcés, B., Navas, A., Machín, J., Stevenson, T., Davis, B., 2000b. Responses of a saline lake ecosystem in a semiarid region to irrigation and climate variability: the history of Salada Chiprana, Central Ebro Basin, Spain. Ambio 29 (6), 344–350.

Van der Knaap, W.O., Van Leeuwen, J.F.N., 1995. Holocene vegetation succession and degradation as responses to climatic change and human activity in the Serra de Estrela, Portugal. Review of Palaeobotany and Palynology 89, 153–211.

Verschuren, D., Laird, K.R., Cumming, B.F., 2000. Rainfall and drought in equatorial east Africa during the past 1,100 years. Nature 403, 410–413.

Wansard, G., Julià, R., Roca, J.-R., Riera, S., Seret, G., 1998. The last 2000 years—environmental change of Lake Estanya (NE Spain) based on mineralogy, ostracod fauna and trace-element shell chemistry. Terra Nostra 98 (6), 132–136.

Yll, E., Pérez-Obiol, R., Pantaleón-Cano, J., Roure, J.M., 1997. Palynological evidence for climatic change and human activity during the Holocene in Minorca (Balearic Islands). Quaternary Research 48, 339–347.

Zorita, E., Kharin, V., von Storch, H., 1992. The atmospheric circulation and sea surface temperature in the North-Atlantic area in winter: their interaction and relevance for Iberian precipitation. Journal of Climate 5, 1097–1108.